

Synthesis and characterization of metal tungstates by novel solid-state metathetic approach

Purnendu Parhi, T.N. Karthik¹, V. Manivannan*

Department of Mechanical Engineering, Campus Delivery 1374, Colorado State University, Fort Collins, CO 80523, USA

Received 8 August 2007; received in revised form 16 October 2007; accepted 20 October 2007

Available online 26 October 2007

Abstract

Novel solid state metathetic approach (SSM) ($ACl_2 + Na_2WO_4 \rightarrow AWO_4 + 2NaCl$, A = Ca, Sr, Ba, Zn, Mn, Ni) assisted by microwave energy has been successfully applied to the synthesis of tungstates of scheelite- and wolframite-type that are of technological importance. Well crystalline phases of scheelite-type tungstates, MWO_4 (M = Ca, Sr, Ba) have been synthesized where the characteristics of SSM reaction and the formation of high lattice energy by-product NaCl drives the reaction toward completion. Among wolframite-type tungstates, single-phase $ZnWO_4$ is synthesized by SSM reactions at ambient conditions and MWO_4 (M = Ni, Mn) are synthesized after subjecting the amorphous product to moderate temperature of heating (around 500 °C for 6 h). This alternative method of synthesis where the metathesis reactions proceed in solid state has features like: simple method of synthesis, cost-effectiveness, high yield, easy scale up, and thus has advantages over already known methods of synthesis. © 2007 Elsevier B.V. All rights reserved.

Keywords: Ceramics; Solid-state reaction; Scanning electron microscopy; X-ray diffraction

1. Introduction

AWO_4 type of compounds (A = bi-valent element) are well known. The most common are the minerals scheelite ($CaWO_4$) used for optical properties (scintillation counters, lasers, optical fibers) and wolframite ($FeWO_4$, $MnWO_4$) which is the most common raw material for producing tungsten metal. In the AWO_4 type of compounds, if A^{2+} has a small ionic radius, $<0.77 \text{ \AA}$ (Mg, Zn) it will form the monoclinic wolframite structure, but larger A^{2+} cations $>0.77 \text{ \AA}$ (Ca, Ba) form the tetragonal scheelite structure. Monoclinic $ZnWO_4$ is also a known material named sanmartinite.

AWO_4 -type have attracted a great deal of interest in the recent years due to their use as laser host materials [1,2], as scintillator [3,4], oxide ion conductors [5], microwave applications [6] and magnetic materials [7]. These tungstate materials doped with rare-earth ions have optical and laser properties.

AWO_4 powders have been prepared by a traditional solid-state reaction [8] and by various wet methods such as

co-precipitation [9], solvo-thermal process [10–12], sol-gel reaction [13], reverse micellar reaction [14], microwave irradiation [15], and mechanochemical method [16]. Ryu et al. have synthesized MWO_4 (M = Ca, Ni) using citrate combustion method [17]. The citrate complex route assisted by microwave has been used by the same group for synthesis of MWO_4 (M = Ca, Sr, Ba, Pb) [18]. Nanocrystalline particle synthesis of MWO_4 (M = Ca, Sr, Ba, Cd, Zn, Pb) has been carried out by Chen et al. using ethylene glycol [19]. Polymethacrylic acid as a template reagent has been used by Zhao et al. for synthesis of $SrWO_4$ hollow sphere [20]. Among these different methods the solution based chemical synthetic methods play a crucial role in the design and production of fine ceramics and have been successful in overcoming many of the limitations of the traditional solid state, high-temperature methods. The use of solution chemistry can eliminate major problems such as long diffusion paths, impurities and agglomeration which will result in products with improved homogeneity.

However, wet methods have disadvantages such as complicated synthetic steps, use of expensive equipment, high synthetic temperature and long sintering time. On the other hand, due to excessive energy consumption, complex apparatus and techniques the solid-state reaction becomes gradually unpopular and unsatisfied. However, solid-state synthesis of materials by

* Corresponding author. Tel.: +1 970 491 2207; fax: +1 970 491 3827.

E-mail address: mani@engr.colostate.edu (V. Manivannan).

¹ Summer intern from IIT, Chennai, India.

metathetic route is emerging as a viable alternative approach to synthesize high-quality novel inorganic materials in a short amount of time.

Solid-state metathetic approach has been successfully applied for the synthesis of many oxide materials. For example, Gopalakrishnan et al. have synthesized oxides of $K_2La_2Ti_3O_{10}$, $Ca_2La_2CuTi_2O_{10}$ belonging to Ruddleson-Popper type of materials, ABO_3 perovskite type of materials like $LaMO_3$ ($M = Co, Mn$), $ATiO_3$ ($A = Ca, Sr$ and Ba) and double perovskites like $Ba_3MM'_{2}O_9$ ($M = Mg, Ni, Zn; M' = Nb, Ta$) by this approach [21–24]. In addition, Kaner et al. have synthesized oxides of Zr, Hf and Cu using this approach [25,26]. Recently we have synthesized $Zn_3(PO_4)_2$ at room-temperature using this procedure [27].

Synthesis of scheelite-type ABO_4 ($A = Ca, Sr, Pb; B = Mo, W$) has been reported by solution-based metathetic approach where the desired product was precipitated after dissolving high purity alkaline earth and lead chloride in distilled water, and adding this solution to the solution of appropriate amounts of sodium molybdate or tungstate [28]. Synthesis of wolframite-type $MnWO_4$ was reported by solution based metathesis reactions, when the precipitate obtained from mixing equimolar solutions of corresponding hydrated metal nitrates and hydrated sodium tungstates was heated to $800^\circ C$ for 15 h [29].

Here we report the synthesis of scheelite-type ABO_4 ($A = Ca, Sr, Ba$) by novel *solid-state metathetic approach* assisted by microwave energy radiation and extended the same approach to the successful synthesis of tungstates of wolframite-type MWO_4 , ($M = Zn$). To the best of our knowledge such an approach towards the synthesis of metal tungstates has not been reported thus far.

2. Experimental

$Na_2WO_4, CaCl_2, SrCl_2, BaCl_2, ZnCl_2, MnCl_2, NiCl_2$ obtained from Alfa Aesar, USA, were used as precursors for the preparation of the metal tungstate compounds. Preparation of calcium tungstate was carried out by reacting a well-ground mixture of $CaCl_2$ and Na_2WO_4 in a molar ratio of 1:1. Sample mixtures were put into crucibles and then exposed to domestic microwave operating at a frequency of 2.45 GHz and a power of 1100 W for 10 min duration. The samples were washed with distilled water to remove the sodium chloride reaction by-product and dried at $80^\circ C$. Preparation of strontium, barium and zinc tungstate powders were carried out in a similar manner by reacting to a well-ground mixture of ACl_2 ($A = Sr, Ba, Zn$) and Na_2WO_4 , as mentioned above. For the synthesis of $MnWO_4$ and $NiWO_4$ the microwave synthesized product after washing is heated at $500^\circ C$ for 6 h.

Powder X-ray diffraction (XRD) measurements were carried out using Scintag X2 diffractometer with $Cu K\alpha$ radiation and Peltier detector. A scan rate of $1^\circ/min$ with a step size of 0.02° was employed to obtain the XRD spectra. Scanning electron microscope (SEM) characterization was performed on the JSM-6500F, a field emission system with the In-Lens Thermal Field Emission Electron Gun (TFEG). Diffuse reflectance (DR) spectra were recorded in the wavelength range 250–2500 nm using Varian Associates Cary 500 double beam spectrophotometer equipped with Praying mantis. X-ray photoelectron spectroscopy (XPS) experiments were performed on a Physical Electronics 5800 spectrometer. This system has a monochromatic $Al K\alpha$ X-ray source ($h\nu = 1486.6 eV$), hemispherical analyzer, and multichannel detector. A low energy (30 eV) electron gun was used for charge neutralization on the non-conducting samples. The binding energy (BE) scales for the samples were referenced to the C 1s peak at 284.8 eV. To determine the SSM reaction final adiabatic temperatures Pyro manufactured calibrated Micro Optical Pyrome-

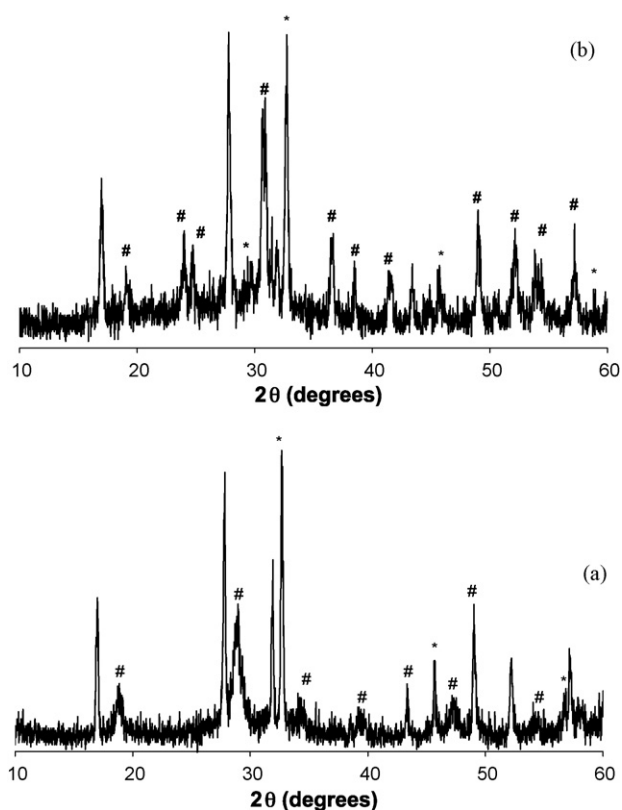


Fig. 1. XRD pattern showing the formation of NaCl (marked *) along with the desired products $CaWO_4$ (marked #) (a) and $ZnWO_4$ (marked #) (b), validating the solid-state metathesis approach of synthesis of making tungstate materials.

ter with the capability to measure reaction temperatures up to $3200^\circ C$ was used.

3. Results and discussion

Fig. 1a shows the powder XRD of scheelite-type calcium tungstate product as a result of solid-state metathesis reaction between calcium chloride and anhydrous sodium tungstate. The XRD pattern contains peaks corresponding to two phases, NaCl (marked with *) and that of metal tungstate (marked with #). The formation of NaCl as a by-product confirms the reaction is characteristic of solid-state metathesis reactions: fast, energetic involving exchange of reacting partners and driven by high lattice energy of the co-produced salt (NaCl), as established in the literature [21–27,30–37]. Microwave radiation has provided the required energy to overcome the energy barrier which precludes spontaneous reaction and helped to heat the bulk of the material uniformly resulting in fine particles of controlled morphology and forming the product in a “green” manner without generation of any solvent wastes.

The as-prepared sample is thoroughly washed with distilled water and dried with acetone to dissolve NaCl and get the desired product $CaWO_4$. XRD (Fig. 2a) showed a well crystalline, single-phase nature for the product with yield >80%. Calcium tungstate crystallizes in tetragonal crystal structure. Scheelite structures of strontium and barium tungstates were synthesized in the method described above and their single-phase nature of

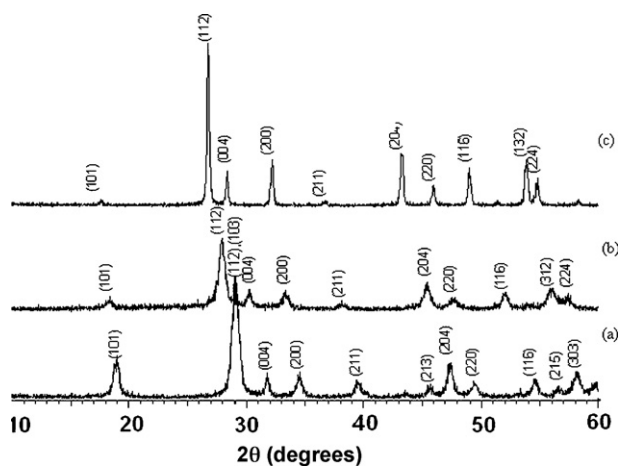


Fig. 2. XRD pattern showing the single-phase formation for scheelite-type (a) CaWO_4 , (b) SrWO_4 , and (c) BaWO_4 .

material is confirmed by XRD (Fig. 2b and c). Crystal structure details about the scheelite-type of tungstates synthesized by solid-state metathesis approach are summarized in Table 1. All the peaks of the XRD are indexed and well matched with the reported phases of JCPDS [38].

SSM approach has been extended to the synthesis of tungstates of wolframite-type as well. Fig. 1b shows the XRD of as-prepared material that contains both NaCl and the desired zinc tungstate phases. Presence of sodium chloride once again confirms the reaction has proceeded in solid-state metathesis way. The desired product is obtained after dissolving sodium chloride and the XRD showed well crystalline single-phase nature with yield >80%. Intensities of the peaks (Fig. 3c) and the cell parameters clearly confirmed the phases belong to wolframite ZnWO_4 (Table 1). For NiWO_4 and MnWO_4 , XRD showed amorphous nature for the as-washed products which were subjected to moderate temperature of heating, i.e. around 500°C for 6 h in air to obtain single-phase crystalline phases (Fig. 3a and b). All the peaks of the XRD are indexed and well matched with the reported phase of JCPDS [39]. The lattice parameters for these compounds are also given in Table 1. It is possible that the formation of amorphous products for Ni and Mn could be due to insufficient and inhomogeneous transfer of microwave energy to form the product. Varying the microwave conditions (power and duration of the reaction), within the limitations of the microwave equipment yielded only amorphous products. It is interesting to note that the previous report of synthesis of such compounds, including that of low temperature methods (except hydrothermal method) [15,28] obtained crystalline product only

Table 1
Crystal structure details of metal tungstates synthesized in this study

Composition	a (Å)	b (Å)	c (Å)	α	β	γ	Volume (Å ³)	Z	Space group
CaWO_4	5.216(0)	5.216(0)	11.313(0)	90	90	90	307.79	4	$I4/a$
SrWO_4	5.376(0)	5.376(0)	11.876(0)	90	90	90	350.66	4	$I4/a$
BaWO_4	5.570(2)	5.570(2)	12.637(0)	90	90	90	400.86	4	$I4/a$
ZnWO_4	4.720(0)	5.700(0)	4.950(0)	90	89.66(7)	90	133.17	2	$P2/c$
MnWO_4	4.798(0)	5.710(6)	4.973(8)	90	91.22	90	136.26	2	$P2/c$
NiWO_4	4.599(2)	5.660(6)	4.906(8)	90	90.03	90	127.74	2	$P2/c$

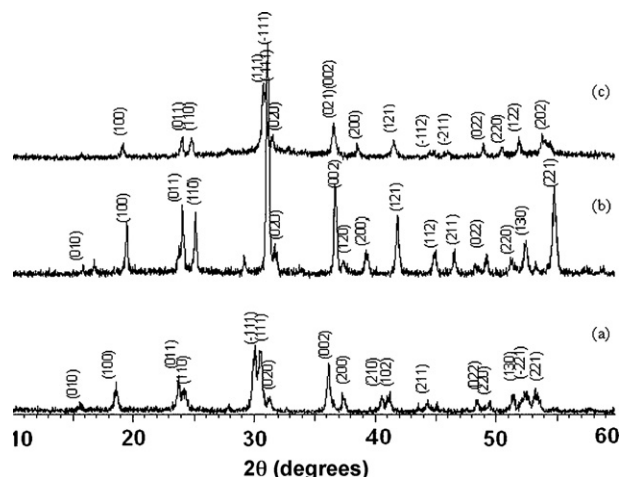


Fig. 3. XRD pattern showing the pure-phase formation of (a) NiWO_4 , (b) MnWO_4 , and (c) ZnWO_4 .

after subjecting the as-prepared product to high-temperature sintering.

3.1. Thermodynamics behind metathesis

Solid state metathesis reactions, an example of which is shown in this study ($\text{ACl}_2 + \text{Na}_2\text{WO}_4 \rightarrow \text{AWO}_4 + 2\text{NaCl}$, $\text{A} = \text{M}^{2+}$) involves exchange of atomic/ionic species, where the driving force being the formation of thermodynamically stable alkali or alkaline earth halides with high lattice energy. Thermodynamic basis for such metathetic reactions are reported in the literature [23,40–42]. SSM reactions are characterized by a large enthalpy change (ΔH_m) and high adiabatic temperature (T_m). The final adiabatic temperature measured was 1623 K for ZnWO_4 . Using thermodynamic data available in the literature [43], we have calculated the enthalpy (ΔH) and free energy changes (ΔG) associated with the formation of tungstates, and presented the result in Table 2. The result show, ($\Delta H -36.17$ KJ/mol for ZnWO_4) that both enthalpy and free energy favors the metathesis reaction and the enthalpy change is indeed the driving force for the metathesis involving the formation of NaCl. We believe the final adiabatic temperature for scheelite tungstates to be below 650°C . Due to restricted wavelength response of the device to the red region of the visible, optical pyrometers can only be used to measure objects that are hot enough to be incandescent or glowing, which limited the lower end of the temperature measurement range of the devices to be about 650°C . SSM

Table 2

Thermodynamic data for CaWO_4 and ZnWO_4 synthesized by metathesis reactions. ΔH_T° and S_T° were calculated using the expression, $\Delta H_T^\circ = \Delta H_{298}^\circ + 298 \int_T^{298} (C_p^\circ/T) dT$ and $S_T^\circ = S_{298}^\circ + 298 \int_T^{298} (C_p^\circ/T) dT$, together with the expression of C_p° as a function of T. ΔG_T° values were calculated by using the expression $\Delta G_T^\circ = \Delta H_T^\circ - T\Delta S_T^\circ$. ΔH_{298}° , S_{298}° , C_p° values were taken from reference [43]

Composition	ZnWO_4
ΔH_{298}° (KJ mol ⁻¹)	-97.8
ΔS_{298}° (KJ mol ⁻¹)	0.0167
ΔG_{298}° (KJ mol ⁻¹)	-102.77
ΔH_T° (KJ mol ⁻¹)	-36.17
ΔS_T° (KJ mol ⁻¹)	0.095
ΔG_T° (KJ mol ⁻¹)	-190.35

reactions occur so rapidly that all of the released enthalpy is essentially used to heat up the solid products, usually raising the alkali halide near or above its normal boiling point and have been recognized as approximately adiabatic in nature [23].

3.2. Characterization of MWO_4 materials

Among scheelite tungstates, SEM showed spherical shape particles for Ca, Sr compounds (Fig. 4a and b) and rod-like features for Ba materials (Fig. 4c). Zn compounds have well defined prism-type morphology and the particles are sub-micron in size (Fig. 4d). For other wolframite tungstates Ni and Mn, SEM showed the particles were agglomerated in nature as shown in Fig. 4e and f.

For tungstate materials to be used as practical phosphor as one of the potential technological applications, a dense pinhole free coating of the same has to be produced on the desired substrate. The quality of coating is determined mainly by the particle size distribution and morphology of the particles. For example, in case of a fluorescent lamp phosphor, the optimum coating thickness is roughly proportional to its mean particle size: that is, the smaller the particle size, the thinner the coating can be. Fine-particle phosphors also yield denser coatings. The well-defined particle features of the tungstates synthesized by SSM reactions showed that these reactions have control over morphol-

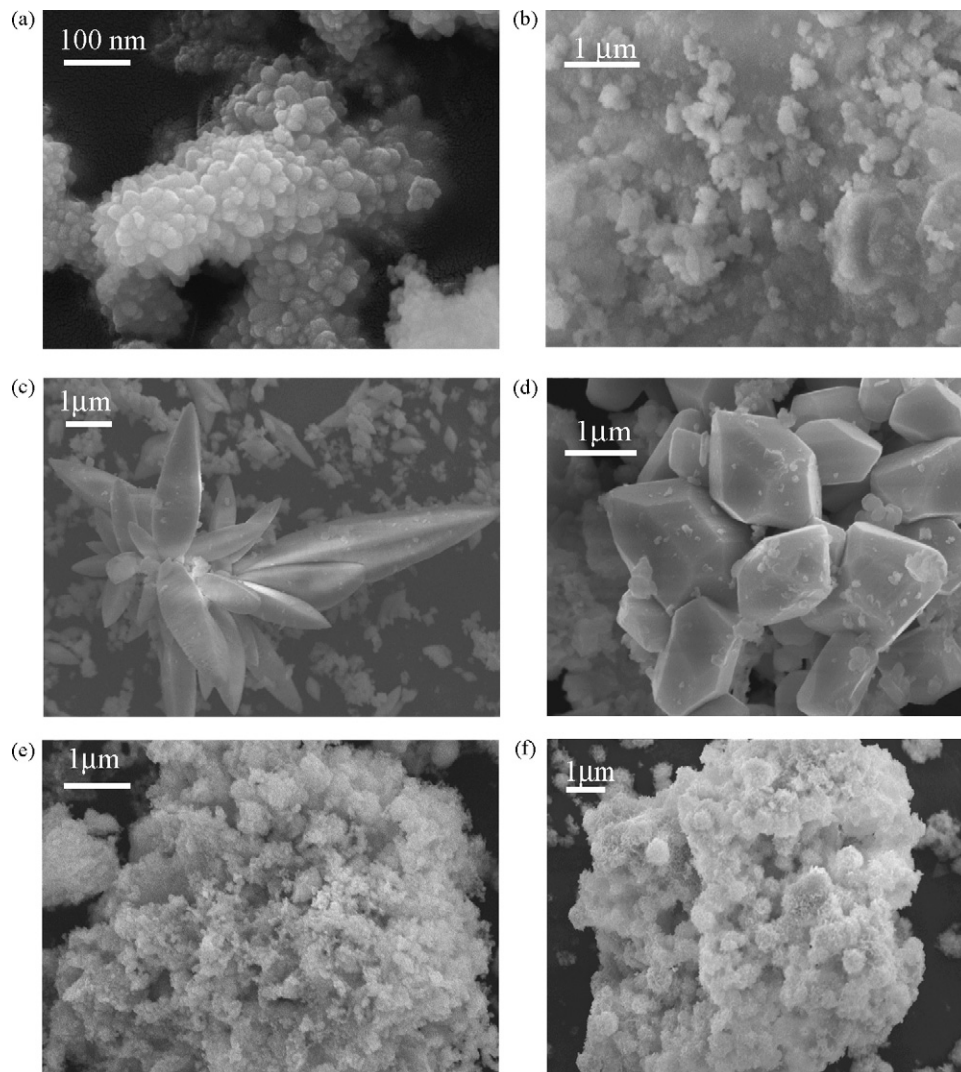


Fig. 4. SEM pictures of (a) CaWO_4 , (b) SrWO_4 , (c) BaWO_4 , (d) ZnWO_4 , (e) MnWO_4 and (f) NiWO_4 showing particle features.

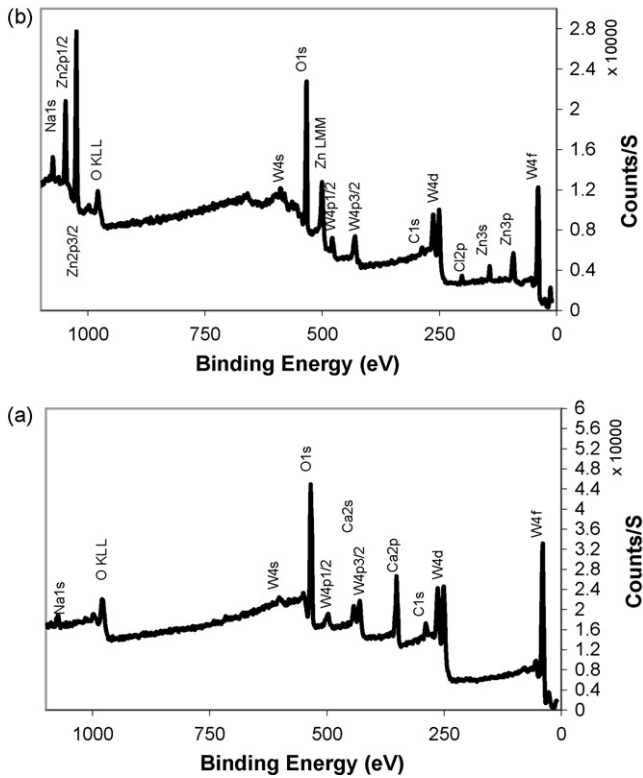


Fig. 5. XPS of (a) scheelite-type (a) CaWO_4 and (b) wolframite-type MnWO_4 .

ogy of the final particles and could be used for such technological applications.

Fig. 5a shows the XPS of CaWO_4 (scheelite) and Fig. 5b shows the XPS of ZnWO_4 (wolframite). XPS provides valuable information concerning the elements in the near surface region. Examination of the binding energies of the core-level electronic states of the elements in the surface region provides qualitative, semi-quantitative and chemical-state information. Since the electron binding energy of elements differs from each other, a full-scan spectrum was given for an overall understanding on surface elemental constituents of the tested sample. In the spectra we can see peaks corresponding to $\text{Ca}2s$ (442.0 eV), $\text{Ca}2p$ (351.6 eV), $\text{W}4s$ (598.2 eV), $\text{O}1s$ (534.8 eV), $\text{W}4d$ (250.8 eV), $\text{W}4f$ (39.6 eV). Similarly in the spectra of ZnWO_4 we can see peaks corresponding to $\text{Zn}2p_{1/2}$ (1047.6 eV), $\text{Zn}2p_{3/2}$ (1024.4 eV), $\text{Zn}3s$ (142.0 eV), $\text{Zn}3p$ (91.6 eV), $\text{W}4s$ (587.6 eV), $\text{W}4p_{3/2}$ (429.2 eV), $\text{W}4p_{1/2}$ (477.2 eV), $\text{W}4d$ (252.0 eV), $\text{W}4f$ (37.6 eV), $\text{O}1s$ (533.2 eV). The $\text{C}1s$ peak at 284.8 eV is due to adventitious carbon present in the surface.

3.3. Physical property measurement of MWO_4 compounds

In order to determine the optical band gap for the technologically important tungstate materials, DR measurements were carried out. Fig. 6a shows the diffuse reflectance spectra of the CaWO_4 , SrWO_4 , BaWO_4 samples in the UV–vis–NIR range whereas Fig. 7a shows the diffuse reflectance spectra of the MnWO_4 , NiWO_4 , and ZnWO_4 . The diffuse reflectance data was

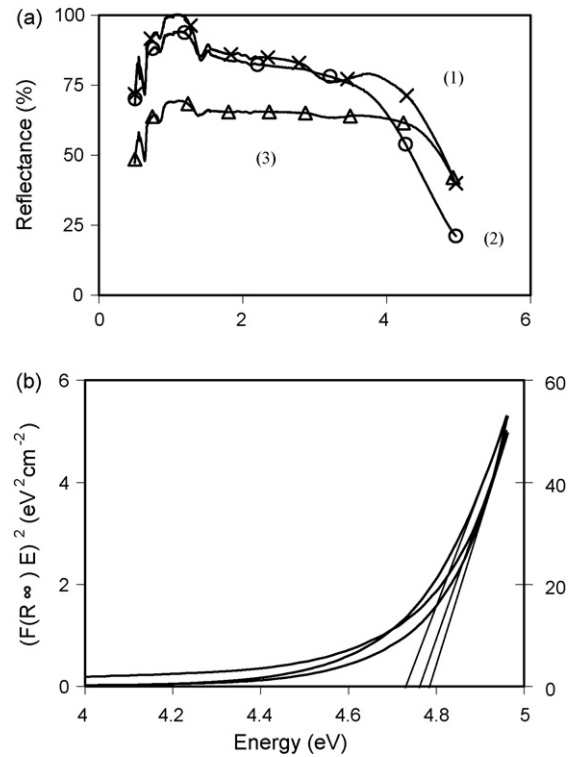


Fig. 6. (a) Diffuse reflectance spectra of (1) CaWO_4 , (2) SrWO_4 , and (3) BaWO_4 in the wavelength range 250–2500 nm. (b) Plot of $F(R_\infty)$ vs. E (eV) for the estimation of the optical absorption edge energy.

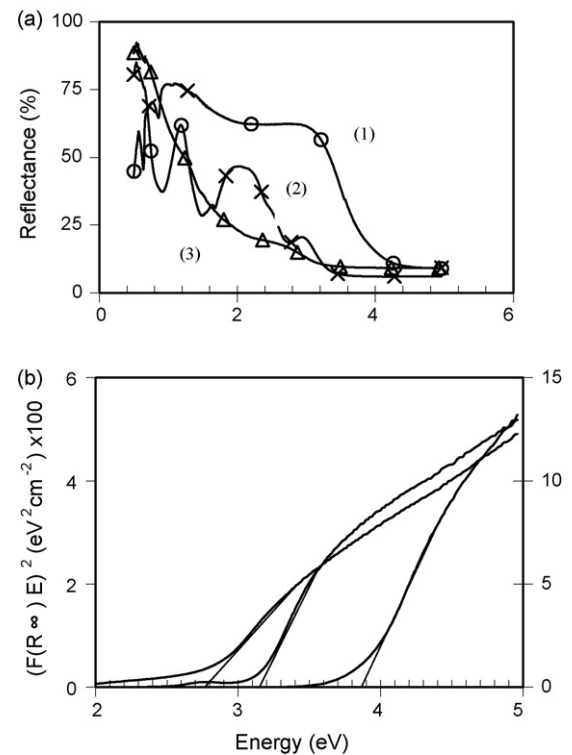


Fig. 7. (a) Diffuse reflectance spectra of (1) ZnWO_4 , (2) NiWO_4 , and (3) MnWO_4 in the wavelength range 250–2500 nm. (b) Plot of $F(R_\infty)$ vs. E (eV) for the estimation of the optical absorption edge energy.

Table 3

Optical absorption edge energies of metal tungstates measured by diffused reflectance techniques

Composition	Band gap (eV)
CaWO ₄	4.75 ± 0.2
SrWO ₄	4.78 ± 0.2
BaWO ₄	4.8 ± 0.2
ZnWO ₄	3.9 ± 0.2
MnWO ₄	2.8 ± 0.2
NiWO ₄	3.2 ± 0.2

used to calculate the absorption coefficient from the Kubelka-Munk [44] function defined as

$$F(R_{\infty}) = \frac{\alpha}{S} = \frac{(1 - R_{\infty})^2}{2R}$$

here α is the absorption coefficient and S the scattering coefficient, and $F(R_{\infty})$ is the KM function. For the diffused reflectance spectra, KM function can be used instead of α for estimation of the optical absorption edge energy [45]. It was observed that a plot of $F(R_{\infty})E$ versus E was linear near the edge for direct allowed transition ($\eta = 1/2$). The intercept of the line on abscissa ($F(R_{\infty})E = 0$) gave the value of optical absorption edge energy. The values are determined to be ~ 4.8 eV for the scheelite tungstates and around 3 eV for wolframite tungstates. Figs. 6b and 7b shows the plot of the same. Table 3 summarizes the optical absorption edge energies for all the tungstates subjected to DR measurements under this study. The diffused reflectance spectra for direct band gap orthorhombic (β) [46] Ta₂O₅ prepared by heating Ta metal in air is also studied for comparison. The value of optical absorption edge energy for indirect allowed transition for Ta₂O₅ was found to be 4.0 ± 0.2 eV, which is consistent with the value reported in the literature [47].

4. Conclusions

Novel *solid-state metathesis* approach has been employed to synthesize technologically important tungstate materials. SEM showed well-defined morphology for most of the tungstates prepared by this method, which have distinct advantages in terms of simplicity, easy scale up, and are relatively inexpensive with high yield. Optical absorption edge energies for the tungstates synthesized in this study have been determined. The thermodynamic factors, which are the fundamental force behind the design of SSM reactions are considered, and the overall enthalpy released in the reaction is calculated.

Acknowledgement

The authors would like to acknowledge Prof. Allan Kirkpatrick, Head of Department, Mechanical Engineering for his continued help, encouragement and support.

References

- [1] M.J. Treadaway, R.C. Powel, Phys. Rev. B 11 (1975) 862–874.
- [2] W. Chen, Y. Inagawa, T. Omatsu, M. Tateda, N. Takeuchi, Y. Usuki, Opt. Commun. 194 (2001) 401–407.
- [3] P. Lecoq, I. Dafinei, E. Auffray, Nucl. Instrum. Methods Phys. Res. 365 (1995) 291–298.
- [4] S. Takai, K. Sugiura, T. Esaka, Mater. Res. Bull. 34 (1999) 193–202.
- [5] V. Nagirnyi, E. Feldbach, L.J. Onsson, M. Kirm, A. Lushchik, Ch. Lushchik, L.L. Nagornaya, V.D. Ryzhikov, F. Savikhiu, G. Svensson, I.A. Tupitsina, Radiat. Meas. 29 (1998) 247–250.
- [6] L.G. Van Uitert, S. Preziosi, J. Appl. Phys. 33 (1962) 2908–2909.
- [7] H. Ehrenberg, H. Weitzel, C. Heid, H. Fuess, G. Witschek, T. Kroener, J. Van Tol, M. Bonnet, J. Phys.: Condens. Matter 9 (15) (1997) 3189–3203.
- [8] G. Blasse, L.H. Brixner, Chem. Phys. Lett. 173 (1990) 409–411.
- [9] E.F. Paski, M.W. Blades, Anal. Chem. 60 (11) (1988) 1224–1223.
- [10] S.-J. Chen, J. Li, X.-T. Chen, J.-M. Hong, Z. Xue, X.-Z. You, J. Cryst. Growth 253 (2003) 361–365.
- [11] F.-S. Wen, X. Zhao, H. Huo, J.-S. Chen, E.-S. Lin, J.-H. Zhang, Mater. Lett. 55 (2002) 152–157.
- [12] L. Zhang, C. Lu, Y. Wang, Y. Cheng, Mater. Chem. Phys. 103 (2007) 433–436.
- [13] M. Bonanni, L. Spanhel, M. Lerch, E. Fcuglein, G. Muciller, Chem. Mater. 10 (1998) 304–310.
- [14] S. Kwan, F. Kim, J. Akana, P. Yang, Chem. Commun. (2001) 447–448.
- [15] J.H. Ryu, J.-W. Yoon, C.S. Lim, W.-C. Oh, K.B. Shim, Ceram. Int. 31 (2005) 883–888.
- [16] V.V. Zyryanov, Inorg. Mater. 36 (2000) 54–58.
- [17] J.H. Ryu, J.-W. Yoon, C.S. Lim, K.B. Shim, Key Eng. Mater. 317 (2006) 223–226.
- [18] J.H. Ryu, J.-W. Yoon, C.S. Lim, K.B. Shim, Electrochem. Solid State Lett. 8 (2005) D15–D18.
- [19] D. Chen, G. Shen, K. Tang, H. Zheng, Y. Qian, Mater. Res. Bull. 38 (2003) 1783.
- [20] X. Zhao, T.L.Y. Chung, X. Zhang, D.H.L. Ng, J. Yu, A. Amer. Ceram. Soc. 89 (2006) 2960–2963.
- [21] J. Gopalakrishnan, T. Sivakumar, K. Ramesha, V. Thangadurai, G.N. Subbanna, J. Am. Chem. Soc. 122 (2000) 6237–6241.
- [22] T. Sivakumar, S.E. Lofland, K.V. Ramanujachary, K. Ramesha, G.N. Subbanna, J. Gopalakrishnan, J. Solid State Chem. 177 (2004) 2635–2638.
- [23] T.K. Mandal, J. Gopalakrishnan, J. Mater. Chem. 14 (2004) 1273–1280.
- [24] R. Mani, N.S.P. Bhuvanesh, K.V. Ramanujachary, W. Green, S.E. Lofland, J. Gopalakrishnan, J. Mater. Chem. 17 (2007) 1589–1592.
- [25] E.G. Gillan, R.B. Kaner, J. Mater. Chem. 11 (2001) 1951–1956.
- [26] J.B. Wiley, E.G. Gillan, R.B. Kaner, Mater. Res. Bull. 28 (1993) 893–900.
- [27] P. Parhi, V. Manivannan, Mater. Res. Bull., in press.
- [28] V. Thangadurai, C. Knittlmayer, W. Weppner, Mater. Sci. Eng. B 106 (2004) 228–233.
- [29] S.M. Montemayor, A.F. Fuentes, Ceram. Int. 30 (2004) 393–400.
- [30] R.E. Treece, J.A. Conklin, R.B. Kaner, Inorg. Chem. 33 (1994) 5701–5707.
- [31] P.R. Bonneau, R.F. Jarvis, R.B. Kaner, Nature 349 (1991) 510–512.
- [32] A.M. Nartowski, I.P. Parkin, M. MacKenzie, A.J. Craven, I. Macleod, J. Mater. Chem. 9 (1999) 1275–1281.
- [33] J.C. Fitzmaurice, A.L. Hector, I.P. Parkin, A.T. Rowley, Phosphorus Sulfur Silicon 101 (1995) 47–55.
- [34] L. Rao, E.G. Gillan, R.B. Kaner, J. Mater. Res. 10 (1995) 353–361.
- [35] T.K. Mandal, J. Gopalakrishnan, Chem. Mater. 17 (2005) 2310–2316.
- [36] P. Parhi, A. Ramanan, A.R. Ray, Mater. Lett. 60 (2006) 218–222.
- [37] P. Parhi, A. Ramanan, A.R. Ray, Mater. Lett. 58 (2004) 3610–3612.
- [38] JCPDS Card No. 77-2234, 08-0490, 72-0746, ICDD, PCPDFWIN v.2.1, JCPDS-International Centre for Diffraction Data, 2000.
- [39] JCPDS Card No. 72,484, 80-134, 73-0554, ICDD, PCPDFWIN v.2.1, JCPDS-International Centre for Diffraction Data, 2000.
- [40] E.G. Gillan, R.B. Kaner, Chem. Mater. 8 (1996) 333–343.
- [41] J.J. Mack, S. Tari, R.B. Kaner, Inorg. Chem. 45 (2006) 4243–4246.
- [42] A.M. Nartowski, I.P. Parkin, M. Mackenzie, A.J. Craven, I. MacLeod, J. Mater. Chem. 9 (1999) 1275–1281.

- [43] M. Binnewies, E. Milke, *Thermochemical Data of Elements and Compounds*, 2nd ed., Wiley-VCH, Weinheim, 2002.
- [44] G. Kortum, *Reflectance Spectroscopy Principles, Methods, Applications*, Spinger-Verlag, New York, 1969.
- [45] D.G. Barton, M. Shtein, R.D. Wilson, S.L. Soled, E. Iglesia, *J. Phys. Chem. B* 103 (1999) 630–640.
- [46] B.R. Sahu, L. Kleinman, *Phys. Rev. B* 69 (2004) 165202.
- [47] W.H. Knausenberger, R.N. Tauber, *J. Electrochem. Soc.* 129 (1973) 927.